Materials and Design 85 (2015) 527–533

Contents lists available at ScienceDirect

Materials and Design

journal homepage: www.elsevier.com/locate/jmad

Microstructure and mechanical property of Ti and Ti6Al4V prepared by an *in-situ* shot peening assisted cold spraying

Xiao-Tao Luo [a], Ying-Kang Wei [a], Yan Wang [a,b], Chang-Jiu Li [a,*]

[a] State Key Laboratory for Mechanical Behavior of Materials, School of Materials Science Engineering, Xi'an Jiaotong University, Xi'an, Shaanxi 710049, China
[b] LERMPS, Université de Technologie de Belfort-Montbéliard, Site de Sévenans, 90010 Belfort Cedex, France

ARTICLE INFO

Article history:
Received 18 March 2015
Received in revised form 28 June 2015
Accepted 2 July 2015
Available online 8 July 2015

Keywords:
Cold spraying
Titanium
in-situ shot peening
Porosity
Deposition efficiency

ABSTRACT

In the current study, for the first time, an *in-situ* shot peening (SP) is introduced into cold spray by mixing large sized stainless steel particles with spraying powders to prepare dense Ti6Al4V (TC4) and commercially pure Ti (CP Ti) deposits. It is attempted that via the *in-situ* hammering by these large sized SP particles, plastic deformation of the previously deposited layers could be greatly enhanced and thereby porosities can be declined. Results show that, as the SP particle proportion increases from 0 to 70 vol.%, porosities of the CP Ti and TC4 coatings decrease from 13.7% and 15.3% to 0.3% and 0.7%, respectively. SEM observations reveal that no SP particle is incorporated into TC4 coatings. A few SP particles (≤2.3 vol.%) are observed in CP Ti coatings due to the relatively low hardness of CP Ti. Only a slight decline trend in deposition efficiency of the CP Ti and TC4 powders is detected as increasing SP content. The *in-situ* SP results in remarkable work hardening. As the SP particle content increases from 0 to 70 vol.%, Vickers microhardness of the CP Ti and TC4 coatings increase from ~143 and 240 $HV_{0.3}$ to ~203 and 427 $HV_{0.3}$, respectively.

© 2015 Elsevier Ltd. All rights reserved.

1. Introduction

Titanium and its alloys have been widely used as aircraft parts, medical implant materials and protective coatings due to their high specific strength, fatigue resistance, biocompatibility and corrosion resistance [1]. Since titanium and its alloys are active and easy to get oxidized, the low processing temperature feature makes cold spraying an effective process to prepare coatings with negligible oxidation from Ti and its alloys [2–14]. On the other hand, residual compressive stress [15], usually developed in cold sprayed coatings, allows cold spray to deposit materials without thickness limitation under optimized spraying conditions.

In recent years, cold sprayed coatings based on Ti and its alloys have been intensively investigated [2–14]. It was found that these coatings always exhibit porous microstructures and poor inter-particle bonding although they are easily deposited [2–8]. The porosity of the cold sprayed coatings based on Ti and its alloys can be up to tens of percent [2–8]. This makes the corrosion resistance [3,4] and mechanical properties [5–7] of the cold sprayed Ti and its alloys much lower than their bulk counterparts. Hussain et al. [3] prepared Ti coating with nitrogen gas (4 MPa, 800 °C) and examined its corrosion behavior in a 3.5 wt.% NaCl solution. Since the coating contained 4.5 vol.% of the interconnected pores, a doubled E_{cor} and a quadruple I_{corr} were detected as compared to the bulk counterpart. Similar results were also reported by Wang and coworkers [4]. Erissou et al. [5] investigated the mechanical properties of the cold sprayed coatings based on Ti6Al4V deposited under series of spraying conditions. Although the coating was heat treated at 1000 °C, the ultimate tensile strength of the Ti6Al4V coating was tested to be only 462 ± 42 MPa (~1100 MPa for bulk counterpart).

Many efforts have been done to densify Ti and Ti-based alloys by optimizing the spraying parameters [3,5,9–12]. Generally, higher particle velocity and temperature are beneficial to obtain denser deposits [16,17]. For the given nozzle, higher gas pressure and temperature lead to higher gas flow velocity and thereby higher particle velocity. Helium is more effective to accelerate the particles than nitrogen [10–12]. The accelerating gas at higher temperature can heat the spraying particles to higher temperature. The particle temperature can be also increased by using preheated powder carrier gas [12]. Generally, to get dense Ti and its alloy coatings by cold spraying, high temperature helium (>800 °C) is necessary although it is more expensive than nitrogen [10–13]. However, due to the high activity of titanium and its alloys, Kim et al. [13] found that, if the Ti particles are heated to relatively high temperatures, *in-situ* oxidation will occur and nanoscale oxide scale will be formed at inter-particle boundary. This leads to a poor inter-particle bonding and thereby deteriorates the mechanical properties of the sprayed coating. In our previous study [14], an *in-situ* hammering/shot peening (SP) effect in cold spray was reported. In cold sprayed coatings, it was found that the previously deposited layer is inevitably deformed by subsequent particle impacts, which usually results in the underlayer of the coating presenting

* Corresponding author.
E-mail address: licj@mail.xjtu.edu.cn (C.-J. Li).

http://dx.doi.org/10.1016/j.matdes.2015.07.015
0264-1275/© 2015 Elsevier Ltd. All rights reserved.

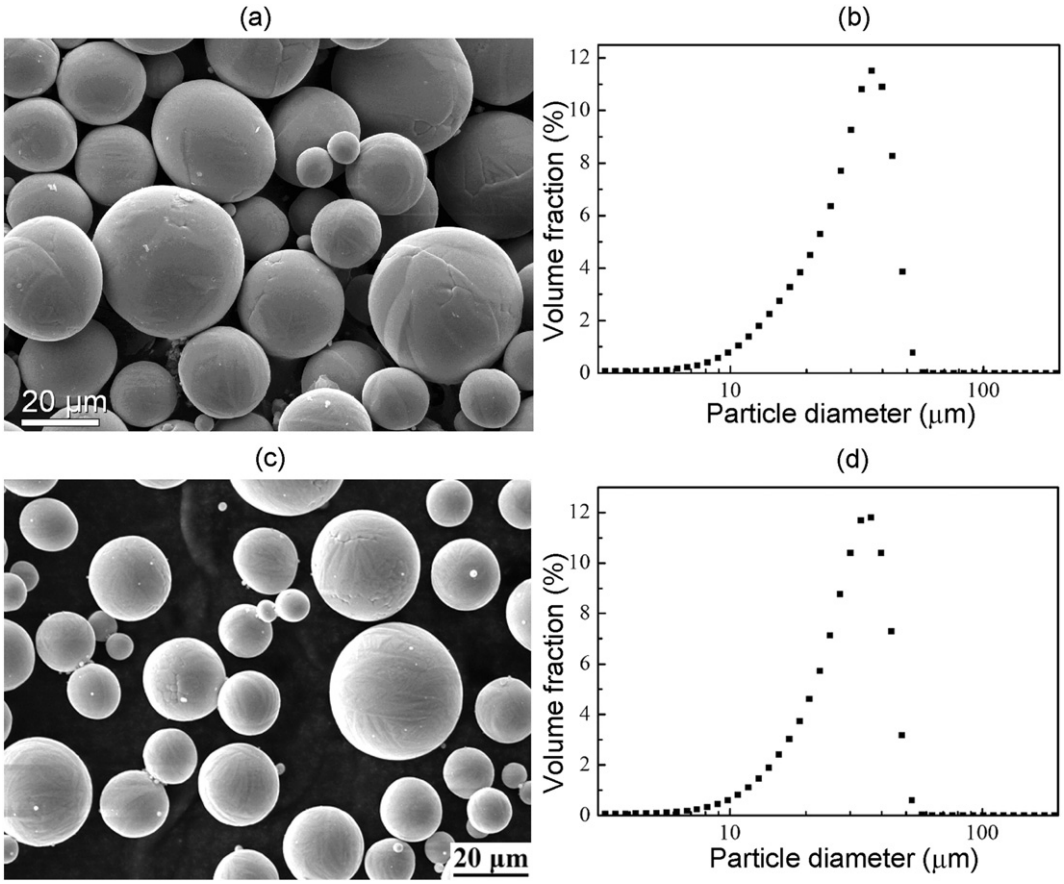

Fig. 1. Morphologies and size distributions of CP Ti and TC4 particles; (a) and (b) correspond to CP Ti and (c) and (d) correspond to TC4.

denser microstructure than the top layer. The *in-situ* densification of following particles to the previously deposited layer is termed as *in-situ* tamping/hammering effect. This phenomenon indicates that the *in-situ* SP/hammering is effective to improve the coating microstructure. However, the *in-situ* hammering by the following impact particle is not powerful enough to achieve a fully dense coating.

It was found that, by adding a certain amount of hard second phase particles into soft Al feedstock [18,19], the porosity of the deposited Al coating can be decreased. However, ceramic particles are easily embedded into the coating due to their low density (high velocity) and angular morphology, which leads to chemical composition changes of the coating material. Meanwhile, some embedded ceramic particles are fractured by the high velocity impact due to their rigid nature and thus deteriorate the coating properties. Because of the pores formed around the fractured ceramic particles, even an increasing trend of porosity as a function of the ceramic particle content was reported by Yandouzi et al. [19]. Bu et al. [20] prepared Al/$Mg_{17}Al_{12}$ composite coating by spraying blended mixture of Al powder and spherical $Mg_{17}Al_{12}$ intermetallic powder. As compared with the coating sprayed with pure Al powder, a dramatic decline in porosity was achieved for Al/$Mg_{17}Al_{12}$ composite coating. The fracture of Al/$Mg_{17}Al_{12}$ particles was absent due to the relatively higher ductility of $Mg_{17}Al_{12}$ than that of ceramics. Meanwhile, no visible pores were observed around the intermetallic particles owning to the spherical morphology of the $Mg_{17}Al_{12}$ particles.

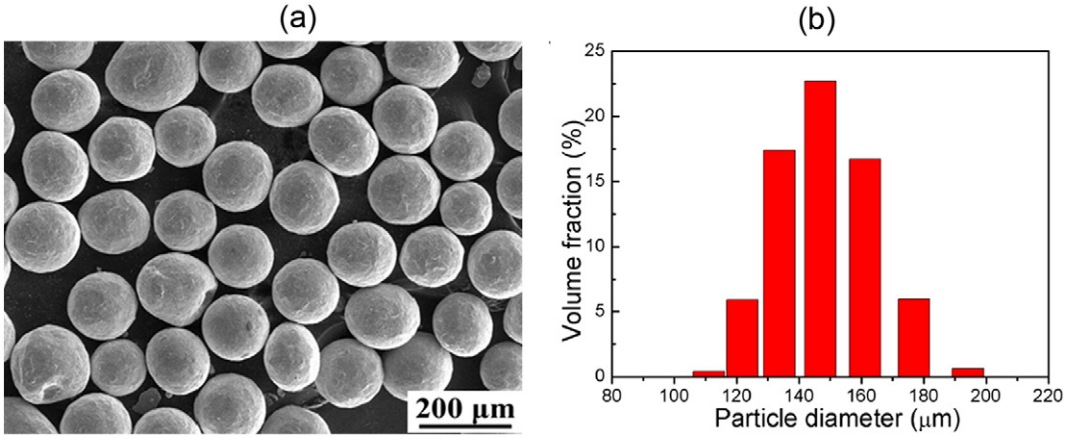

Fig. 2. Morphology (a) and size distribution (b) of 1Cr13 SP particles.

Table 1
Cold spraying parameters.

Gas	Gas temperature (°C)	Gas pressure (MPa)	Gun traverse speed (mm/s)	Standoff distance (mm)	Powder feeder rate (g/min)
N_2	550	2.8	40	20	23

In the current study, enhanced *in-situ* hammering is introduced by blending large sized stainless steel SP particles with the spraying powders. It is attempted that via the *in-situ* hammering by those large sized SP particles, plastic deformation of the deposited CP Ti and TC4 layers can be greatly enhanced and thereby porosity of the deposit can be reduced.

2. Experimental procedures

2.1. Materials

Gas atomized Ti6Al4V (TC4) and commercially pure Ti (CP Ti) powders were used as the spraying powders. As can be seen from Fig. 1, both TC4 and CP Ti particles reveal spherical morphology. Sizes of the CP Ti particles range from ~10 to ~50 μm with an average value of 31.7 μm. TC4 powder is slightly smaller than CP Ti powder and has an average diameter of 29.3 μm.

As shown in Fig. 2, a spherical shaped 1Cr13 stainless steel powder with a narrow particulate size distribution from 120 to 180 μm ($d_{0.5} = 155.7$ μm) was used as the shot peening (SP) particle. To clarify the effect of the SP particle content on microstructure and mechanical properties of the cold sprayed coatings, 10 vol.%, 30 vol.%, 50 vol.% and 70 vol.% of the SP particles were mixed into the CP Ti and TC4 powders, respectively. These powder mixtures were used as the feedstocks for coating deposition. 1Cr18Ni9 stainless steel plates with a thickness of 3 mm were used as the substrates. These plates were grit blasted prior to the coating deposition to produce rough surfaces.

2.2. Coating deposition

An in-house made cold spray system was used for coating deposition. In this system, the spray powders are fed into the nozzle along the axis. A convergent–divergent Laval nozzle, which is made of WC–Co cermet, was used with a throat diameter of 2.7 mm, an outlet diameter of 6 mm and a divergent section length of 150 mm. Nitrogen was used as the accelerating gas and powder carrier gas. Detailed spraying parameters are listed in Table 1.

For comparison, CP Ti and TC4 were also deposited with helium gas under the same conditions. Because of the different thermodynamic properties of both gases, the same spray parameters may lead to the formation of shockwaves in one gas but not the other. According to the simulation results reported by Jodoin [21], for a given nozzle, shockwave is more likely to be formed in helium gas flow than in nitrogen because of the higher Mach number of helium. Meanwhile, the shockwave has a noticeable effect on particle velocity, especially for small/light particles. In this study, shockwaves were formed in both cases. Impact velocities of CP Ti, TC4 and the SP particle were estimated by fluid dynamics simulation approach. The interaction between the SP particles and the spraying particles within the gas flow was not taken into account. Details about the simulation procedure can be referred elsewhere [22].

2.3. Microstructure characterization and microhardness measurement

Scanning electron microscopy (SEM) was carried out to characterize the microstructure of the sprayed coatings. Energy dispersive spectroscopy (EDS), attached in SEM system, was employed to analyze the chemical composition of the sprayed coatings. The sawed samples were firstly mounted into epoxy resin, then ground by SiC abrasive paper after they were solidified and finally polished by a 0.1 μm diamond polish agent. To minimize the effect of smearing on the measured porosity value, the samples were further polished by an ultrasonic vibration polisher for 1 h with a 50 nm sized alumina polish agent. The samples were then ultrasonically cleaned twice in an ethanol bath for 5 min to remove the adhered polish agent. Porosities of the sprayed samples were measured from their polished cross sections based on image analysis. For each sample, 10 SEM images taken at 1000× in back scattered electron (BSE) were used. In BSE mode, the pores and cracks are in dark contrast while CP Ti and TC4 present bright contrast. The porosity value equals to the ratio of the pixel of the dark region to that of the entire cross section. To evaluate the effect of the *in-situ* SP on deposition behavior of the CP Ti and TC4 powders, deposition efficiency of each powder mixture was measured. In the test, the sample weight was measured by an electronic balance (0.1 mg).

Vickers microhardness test was carried out to evaluate the mechanical properties of the sprayed specimens. For each sample, 10 indentations were made on the polished cross section of each coating with a load of 300 g and a holding of 30 s.

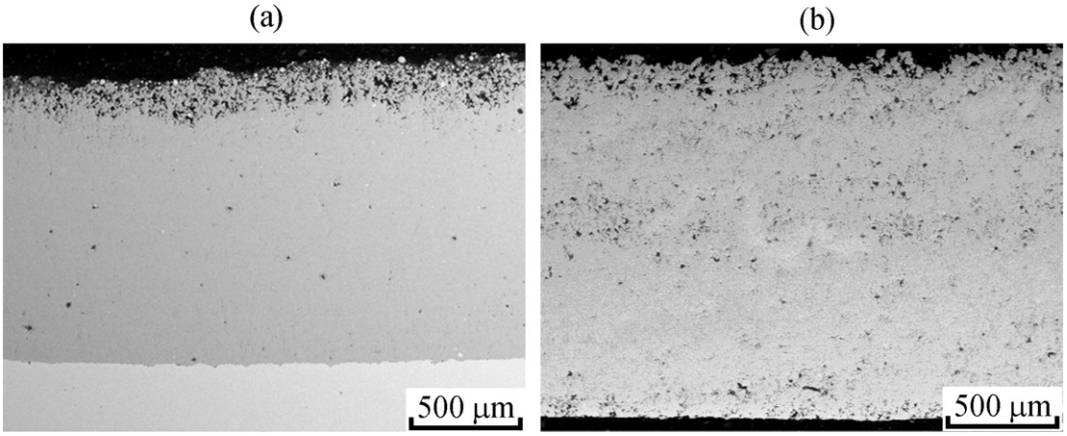

Fig. 3. Cross sectional microstructures of (a) CP Ti and (b) TC4 coatings sprayed with helium gas.

Table 2
Deposition efficiency, porosity and Vickers microhardnesses of the coatings sprayed with helium.

Materials	Porosity (%)	Deposition efficiency (%)	Vickers microhardness ($HV_{0.3}$)
CP Ti	1.3	89.6	192
TC4	2.7	83.7	363

3. Results and discussion

3.1. CP Ti and TC4 deposited with helium

Fig. 3 shows the cross sectional microstructure of the CP Ti and TC4 coatings sprayed with helium gas. CP Ti and TC4 coatings with relatively dense microstructure can be observed. Meanwhile, both coatings show dense under-layer and porous top layer because of the hammering effect. The measured deposition efficiencies of the spraying powders, porosities and Vickers microhardnesses of those two coatings are listed in Table 2. These values are comparable with those in literature [11–13].

3.2. Microstructure of the CP Ti and TC4 coatings deposited by the in-situ SP assisted cold spray

Fig. 4 shows the cross sectional microstructure of the CP Ti coatings deposited with the powders containing different proportions of the SP particles. As expected, the coating deposited by pure Ti powder exhibits a porous microstructure. As can be seen from the close view, most of the CP Ti particles present spherical shape indicating that they underwent little plastic deformation. With the increase in SP particle content, the sprayed CP Ti becomes denser and denser. As the SP particle increases to 70 vol.%, a fully dense coating was obtained and evident pores could not be observed anymore. Meanwhile, as marked with the black arrows, some particles in bright contrast can be observed in the CP Ti deposits. EDS analysis demonstrated that these particles are 1Cr13 stainless steel SP particles. The original spherical shape of these incorporated SP particles was retained indicating that the high velocity impact-induced plastic deformation mainly occurred in CP Ti particles. As the SP particle content increased, more SP particles were incorporated into the deposits. As the SP particle content in feedstock increases to 70 vol.%, the proportion of the SP particles was measured to be 2.4 vol.% in the CP Ti coating.

As is presented in Fig. 5, similar trend can be found in cold sprayed TC4 coatings. A gradual decline in the porosity of the coating can be observed with increasing SP particle content in the feedstocks. However, 1Cr13 SP particle inclusion is absent in TC4 deposit in all cases.

The inclusion of SP particles into the CP Ti coatings is undesirable and unexpected. In cold spraying, adiabatic shear instability (ASI) has been understood as one of the dominant mechanisms for successful bonding of the particles to the substrate or the previously deposited layer. The ASI leads to a sudden rise in the temperature at particle/substrate interface. The high interfacial temperature combined with high level of shear/compressive stress induced by the high velocity impact accounts for the metallurgical bonding between the particle and the substrate. Therefore, the adiabatic shear instability has been frequently used to estimate the critical velocity. Based on this concept, Bae et al. [23] investigated the particle/substrate interface bonding of different material combinations and estimated the critical velocities for various metal combinations. Impact velocities and kinetic energies of the SP particle, CP Ti and TC4 particles were calculated following the approach proposed by Wu et al. [24] under the given conditions (Table 1). The calculated results as well as the physical parameters of the feedstocks are listed in Table 3. The average impact velocity of the SP particles is only 313 m/s which is much lower than the critical velocity for successful bonding of stainless steel particles at comparable temperatures reported in literature [23,25]. According to the classification proposed by Bae et al. [23] and King et al. [26], impact of 1Cr13 SP particle onto CP Ti or TC4 falls into hard particle/soft substrate case. In this case, the adiabatic shear instability plastic deformation preferentially occurs in soft substrate. Meanwhile, it was also found that high mass density and low specific heat are instrumental to the adiabatic shear instability [23]. However, as can be seen in Table 3, although CP Ti and TC4 have comparable densities, specific heat, SP particles were only observed in CP Ti coatings. Hence, the inclusion of the SP particles in Ti coating cannot be attributed to the adiabatic shear instability induced inter-particle bonding.

King et al. [26] found that when the particle material is of significantly higher density and strength than the substrate, penetration of the particle below the substrate surface takes place without rebounding. In this study, as can be seen from Table 3, higher hardness of TC4 than CP Ti makes penetration of 1Cr13 particles into CP Ti much easier than into TC4. Therefore, 1Cr13 SP particle inclusion was only observed in CP Ti coatings. In studies of high-velocity impact, a number of empirical relationships have been proposed, relating basic particle and substrate properties such as density, yield strength or hardness, to crater depth or volume. A positive relation was found between the ratio of crater depth to crater diameter (r) and the impact velocity. Meanwhile, r was found to be linearly related to $(E_p/E_s)(\rho_p/\rho_s)^{0.5}$, where E_p and E_s

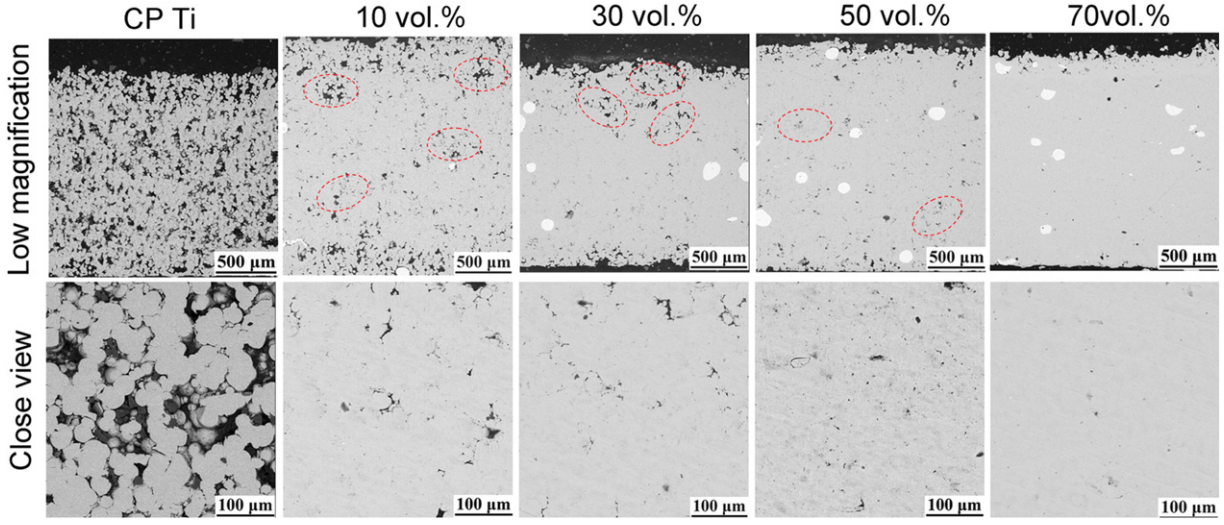

Fig. 4. Cross sectional microstructures of the TC4 coatings deposited with pure TC4 powder and powder mixtures with different proportions of the SP particles.

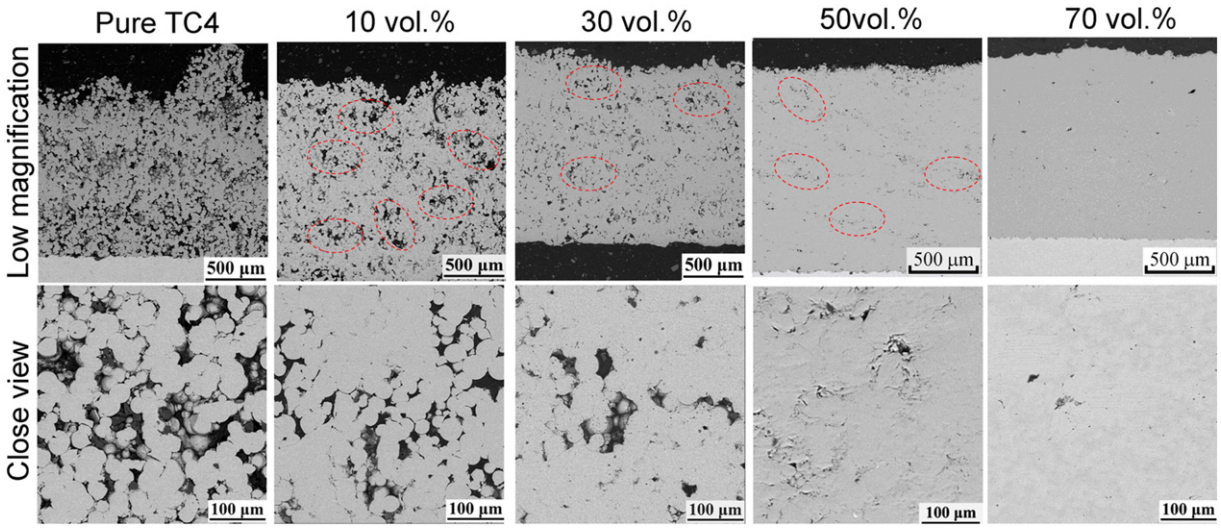

Fig. 5. Cross sectional microstructures of the TC4 coatings deposited with pure TC4 powder and powder mixtures with different proportions of the SP particles.

are the elastic modulus of the particle and substrate, respectively, and ρ_p and ρ_s the densities [27]. It is noted that a higher r suggests a greater probability for SP particle inclusion. This fact suggests that, to avoid the SP particles induced contamination, SP particles of larger size can be used to decrease the impact velocity. Powders of other materials with relatively low elastic modulus or/and low densities can be selected as the SP particles.

It can be also found from Figs. 4 and 5 that the coatings sprayed with the mixed powders containing 10–50 vol.% of the SP particles exhibit heterogenous microstructures. As indicated by the dashed line ellipses, island-shaped porous regions, where the particles underwent little plastic deformation, are dispersed in the coatings. To make it clear, surface morphologies of CP Ti deposits were characterized by SEM. Fig. 6 shows the top-view surface morphologies of the CP Ti deposits sprayed with mixed powders showing the SP particle induced plastic deformation traces. As marked with the arrows, the SP particle impact induced craters can be easily recognized. The diameters of the craters range from ~150 to ~250 μm which are slightly larger than those of the SP particles. The number of the craters increases with increasing SP particle content. However, as the SP particle content ranges from 10% to 50%, the craters cannot cover the entire surface. The regions in/nearby the craters were hammered and densified leaving other regions revealing porous microstructure. As is shown in Fig. 6d, 70 vol.% of SP particle is enough to hammer the entire surface so that fully dense deposit can be obtained (Figs. 4 and 5). Furthermore, because of the hammering effect by the *in-situ* SP, porous top layer, usually observed in coatings deposited by pure Ti/TC4 powders, was absent (Figs. 4 and 5).

Porosities of the sprayed samples were measured by image analysis from polished cross sections of the samples. The porosities of CP Ti and TC4 coatings as a function of the SP particle content are plotted in Fig. 7. The porosities decline rapidly at first and then slowly with increasing SP particle content. As indicated by the dashed lines, CP Ti and TC4 deposited with the powder mixtures containing 50 vol.% of SP particles show comparable porosities with those sprayed with helium gas. As the SP particle content increases to 70 vol.%, the porosities of CP Ti and TC4 coatings are decreased to 0.3% and 0.7%, respectively.

Fig. 8 shows the influence of the SP particle content on deposition efficiencies of the CP Ti and TC4 powders. The powder sprayed with helium gas has the highest deposition efficiency due to the highest particle velocity. As expected, downwards trend with the increase in SP content for both CP Ti and TC4 can be observed. Pure CP Ti powder and TC4 powder yielded the highest deposition efficiencies of 85% and 81%, respectively. When the feedstock contains as many as 70 vol.% of the SP particles, acceptable deposition efficiencies of 73% and 67% for CP Ti and TC4, respectively, were achieved.

In cold spray process, particles of velocities lower than the critical velocity will inevitably blast and remove the deposited layer. In this case, it was found that the rebounded particle induced erosion is enhanced with increasing particle velocity [25]. Therefore, under the same spraying conditions, spray powders containing more large sized particles always result in lower deposition efficiency. In cold spraying, the particle velocity decreases significantly with the increase in particle size and density [17,25]. As can be seen from Table 3, due to the larger size and approximately doubled density as compared to CP Ti and TC4 powders, the average velocity of the SP particles is only 313 m/s, which weakens the erosion to the deposited CP Ti and TC4. Although the SP particles have low velocities, the large mass makes SP particles have enough kinetic energy to densify the deposited CP Ti and TC4. On the other hand, the spherical shape of the SP particles also contributes to the relatively high deposition efficiency. Cold spraying powder mixtures of metallic powder and large sized ceramic powder has been frequently used to prepare composite coatings [28,29]. During coating deposition, sharp edges of the ceramic particles will chip off the deposited metallic particles and remove the weak bonded metallic particles, so that the deposition efficiency dramatically declines with increasing ceramic particle proportion. Meanwhile, ceramic particles with sharp edges are easily embedded and incorporated into the metallic layer. Similar result was also observed in our previous study [30]. In this

Table 3
Physical parameters [22], impact velocities and kinetic energies of the feedstocks.

Powder	Density (g/cm^3)	Specific heat (J/kg·K)	Elastic modulus (GPa)	Hardness ($HV_{0.05}$)	Calculated impact velocity (m/s)	Calculated kinetic energy of single particle (μJ)
CP Ti	4.51	528	116.3	117	682	17.5
TC4	4.43	585	113.2	214	695	13.7
1Cr13 SP	7.87	502	199.9	396	313	767.9

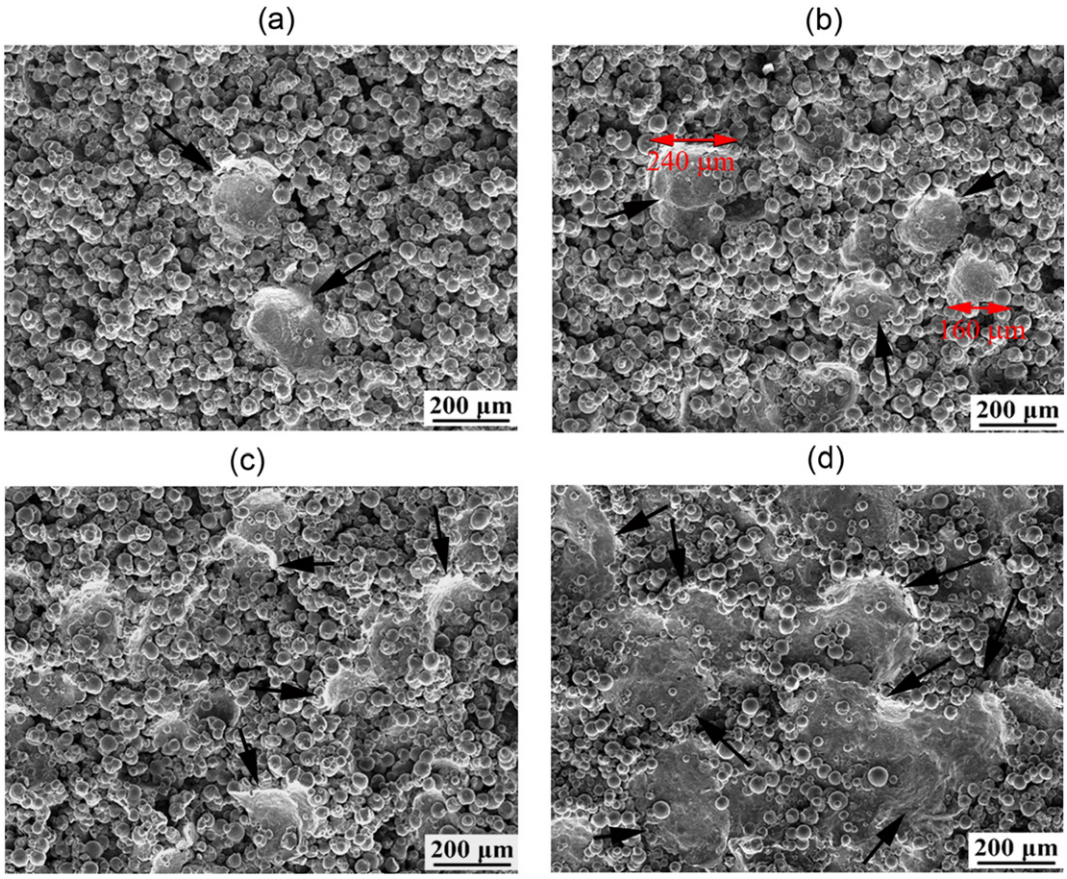

Fig. 6. Surface morphologies of CP Ti deposits sprayed by the *in-situ* SP assisted cold spraying showing the craters induced by SP particle impact; (a), (b), (c) and (d) correspond to coatings prepared with the powders containing 10%, 30%, 50% and 70% of the SP particles, respectively.

sense, spherical morphology of the SP particles benefits high deposition efficiency and low contamination. As a consequence, although 70 vol.% of the SP particles are blended into the spray powders, the relatively large size and spherical morphology of the SP particles led to only a slight decrease in deposition efficiency.

It can be found from Fig. 9 that the coating hardness increases gradually with increasing SP particle content. As the content of the SP particles in feedstock increases to 70 vol.%, the hardness of the sprayed coatings is as twice as that sprayed with pure CP Ti and TC4 powders. The increment in hardness is due to the gradually enhanced work hardening and decreasing coating porosity. It was found that, for the coatings prepared with powders containing less than 30 vol.% of the SP particles, the morphology of the hardness indentations is remarkably affected by the pores. Consequently, the lower hardness values of the pure, 10% and 30% CP Ti and TC4 coatings can be mainly attributed to their relatively high porosity.

4. Conclusions

In this study, to obtain dense CP Ti and TC4 coatings, an *in-situ* SP assisted cold spraying was proposed by blending large sized SP particles into the spray powders. Effect of the SP particle content on coating porosity, deposition efficiency as well as hardness was investigated.

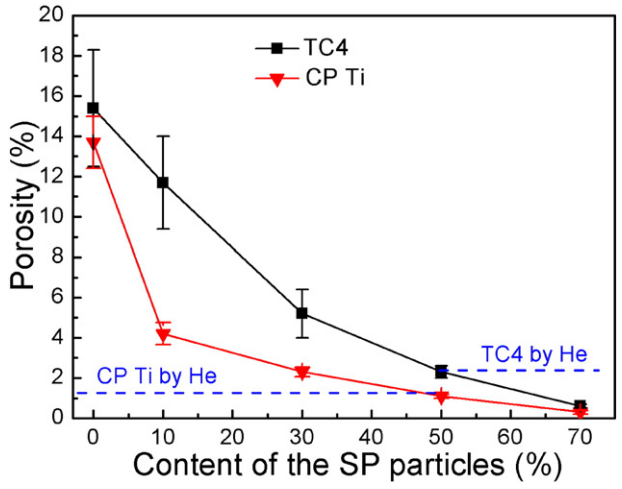

Fig. 7. Porosities of CP Ti and TC4 coatings as a function of the SP particle content.

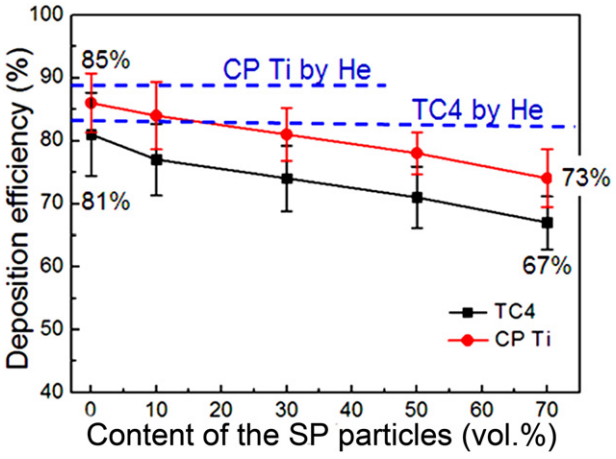

Fig. 8. Deposition efficiencies of the powder mixtures as a function of the SP content.

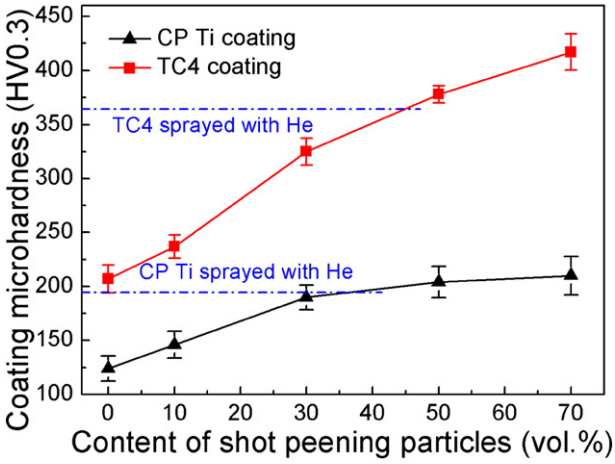

Fig. 9. Vickers microhardness of CP Ti and TC4 coatings as a function of the SP particle content.

The *in-situ* SP assisted cold spray is an effective approach to deposit dense Ti and TC4 coatings. As the SP particle proportion increases from 0 to 70 vol.%, porosities of the CP Ti and TC4 coatings decrease from 13.7% and 15.3% to 0.3% and 0.7%, respectively. Although 70 vol.% of the large sized 1Cr13 SP particles were mixed into the spraying powders, severe erosion does not occur and relatively high deposition efficiencies of 73% and 67% for CP Ti and TC4, respectively, are achieved. Inclusion of 1Cr13 SP particles is not observed in TC4 coatings. As the powder mixture contains 70 vol.% of the SP particles, 2.3 vol.% of SP particles is observed in CP Ti coatings due to the relatively low hardness of CP Ti. Meanwhile, the SP particle hammering induced remarkable work hardening is detected in both CP Ti and TC4 coatings. The *in-situ* shot peening assisted method opens a new way to prepare fully dense Ti and its alloy coatings by cold spraying allowing using of inexpensive nitrogen.

A SP particle recovering device made up of several electromagnet units, by which the *in-situ* SP assisted cold spray will be more economical, is now being developed. Although the deposition efficiency is not significantly reduced, blending of SP particles into spray particles will reduce the amount of coating material sprayed towards the substrate per unit time.

Acknowledgments

The authors would like to thank the financial support by the National Science Fund of China (No. 51401158) and China Postdoctoral Science Foundation (No. 2014M550486).

References

[1] I.J. Polmear, Light Alloys, From Traditional Alloys to Nanocrystals4th ed., 2005. 299–365.
[2] R.E. Blose, B.H. Walker, R.M. Walker, S.H. Froes, New opportunities to use cold spray process for applying additive features to titanium alloys, Met. Powder Rep. 61 (2006) 30–37.
[3] T. Hussain, D.G. McCartney, P.H. Shipway, T. Marrocco, Corrosion behavior of cold sprayed titanium coatings and free standing deposits, J. Therm. Spray Technol. 20 (2011) 260–274.
[4] H.R. Wang, W.Y. Li, L. Ma, J. Wang, Q. Wang, Corrosion behavior of cold sprayed titanium protective coating on 1Cr13 substrate in seawater, Surf. Coat. Technol. 201 (2007) 5203–5206.
[5] P. Vo, E. Irissou, J.G. Legoux, S. Yue, Mechanical and microstructural characterization of cold-sprayed Ti–6Al–4V after heat treatment, J. Therm. Spray Technol. 22 (2013) 954–964.
[6] D. Goldbaum, R.R. Chromik, S. Yue, E. Irissou, J.G. Legoux, Mechanical property mapping of cold sprayed Ti splats and coatings, J. Therm. Spray Technol. 20 (2011) 486–496.
[7] Z.M. Li, X.P. Yang, J.B. Zhang, B.L. Zheng, Y.Z. Zhou, A.D. Shan, E.J. Lavernia, Microstructure evolution and mechanical behavior of cold-sprayed bulk nanostructured titanium, Metall. Mater. Trans. A 45A (2014) 5017–5028.
[8] M. Gardon, A. Latorre, M. Torrell, S. Dosta, J. Fernández, J.M. Guilemany, Cold gas spray titanium coatings onto a biocompatible polymer, Mater. Lett. 106 (2013) 97–99.
[9] W. Wong, P. Vo, E. Irissou, A.N. Ryabinin, J.G. Legoux, S. Yue, Effect of particle morphology and size distribution on cold-sprayed pure titanium coatings, J. Therm. Spray Technol. 22 (2013) 1140–1153.
[10] W. Wong, E. Irissou, A.N. Ryabinin, J.G. Legoux, S. Yue, Influence of helium and nitrogen gases on the properties of cold gas dynamic sprayed pure titanium coatings, J. Therm. Spray Technol. 20 (2011) 213–226.
[11] S.H. Zahiri, C.I. Antonio, M. Jahedi, Elimination of porosity in directly fabricated titanium via cold gas dynamic spraying, J. Mater. Process. Technol. 209 (2009) 922–929.
[12] G. Bae, S. Kumar, S. Yoon, K. Kang, H. Na, H.J. Kim, C. Lee, Bonding features and associated mechanisms in kinetic sprayed titanium coatings, Acta Mater. 57 (2009) 5654–5666.
[13] K.H. Kim, S. Kuroda, Amorphous oxide film formed by dynamic oxidation during kinetic spraying of titanium at high temperature and its role in subsequent coating formation, Scr. Mater. 63 (2010) 215–218.
[14] C.J. Li, W.Y. Li, Deposition characteristics of titanium coating in cold spraying, Surf. Coat. Technol. 167 (2003) 278–283.
[15] G. Shayegan, H. Mahmoudi, R. Ghelichi, J. Villafuerte, J. Wang, M. Guagliano, H. Jahed, Residual stress induced by cold spray coating of magnesium AZ31B extrusion, Mater. Des. 60 (2014) 72–84.
[16] M. Grujicic, C.L. Zhao, W.S. DeRosset, D. Helfritch, Adiabatic shear instability based mechanism for particles/substrate bonding in the cold-gas dynamic-spray process, Mater. Des. 25 (2004) 681–688.
[17] W.Y. Li, H. Liao, G. Douchy, C. Coddet, Optimal design of a cold spray nozzle by numerical analysis of particle velocity and experimental validation with 316L stainless steel powder, Mater. Des. 28 (2007) 2129–2137.
[18] E. Sansoucy, P. Marcoux, L. Ajdelsztajn, B. Jodoin, Properties of SiC-reinforced aluminum alloy coatings produced by the cold gas dynamic spraying process, Surf. Coat. Technol. 202 (2008) 3988–3996.
[19] H. Bu, M. Yandouzi, C. Lu, D. MacDonald, B. Jodoin, Cold spray blended Al + Mg17Al12 coating for corrosion protection of AZ91D magnesium alloy, Surf. Coat. Technol. 207 (2012) 155–162.
[20] M. Yandouzi, P. Richer, B. Jodoin, SiC particulate reinforced Al–12Si alloy composite coatings produced by the pulsed gas dynamic spray process: microstructure and properties, Surf. Coat. Technol. 203 (2009) 3260–3270.
[21] B. Jodoin, Cold spray nozzle Mach number limitation, J. Therm. Spray Technol. 11 (2002) 496–507.
[22] W.-Y. Li, C.-J. Li, Optimization of spray conditions in cold spraying based on the numerical analysis of particle velocity, Trans. Nonferrous Met. Soc. China 14 (2004) 43–48.
[23] G. Bae, Y. Xiong, S. Kumar, K. Kang, C. Lee, General aspects of interface bonding in kinetic sprayed coatings, Acta Mater. 56 (2008) 4858–4868.
[24] J. Wu, H. Fang, S. Yoon, H. Kim, C. Lee, Measurement of particle velocity and characterization of deposition in aluminum alloy kinetic spraying process, Appl. Surf. Sci. 252 (2005) 1368–1377.
[25] T. Schmidt, F. Gärtner, H. Assadi, H. Kreye, Development of a generalized parameter window for cold spray deposition, Acta Mater. 54 (2006) 729–742.
[26] P.C. King, S.H. Zahiri, M. Jahedi, Focused ion beam micro-dissection of cold-sprayed particles, Acta Mater. 56 (2008) 5617–5626.
[27] L.E. Murr, S.A. Quinones, E.T. Ferreyra, A. Ayala, O.L. Valerio, F. Hörz, R.P. Bernhard, The low-velocity-to-hypervelocity penetration transition for impact craters in metal targets, Mater. Sci. Eng. A 256 (1998) 166–182.
[28] Q. Wang, N. Birbilis, H. Huang, M.X. Zhang, Microstructure characterization and nanomechanics of cold-sprayed pure Al and Al–Al_2O_3 composite coatings, Surf. Coat. Technol. 232 (2013) 216–223.
[29] W.Y. Li, C. Yang, Liao H, Effect of vacuum heat treatment on microstructure and microhardness of cold-sprayed TiN particle-reinforced Al alloy-based composites, Mater. Des. 32 (2011) 388–394.
[30] X.T. Luo, C.-J. Li, Large cubic BN reinforced nanocomposite coating with improved wear resistance prepared by cold spraying, Mater. Des. 36 (2015) 249–256.